Determination of laser shock treatment conditions for fatigue testing of Ni-based superalloys

Philippe Forget, Michel Jeandin, A. Lyoret

JOURNAL DE PHYSIQUE IV
Colloque C7, supplément au Journal de Physique III, Volume 3, novembre 1993

Determination of laser shock treatment conditions for fatigue testing of Ni-based superalloys

P. FORGET, M. JEANDIN and A. LYORET*

Ecole des Mines de Paris, Centre des Matériaux P.M. Fourt, BP. 87, 91003 Evry cedex, France
** SNECMA, Centre de Corbeil, Département "Matériaux et Procédés", BP. 81, 91003 Evry cedex, France*

Abstract.

It is envisaged that laser shock surface treatment may be used to surface harden and improve the mechanical properties of materials by inducing compressive stresses. This study deals with its application to the high performance aeronautical Ni-based superalloy Astroloy for turbine discs and its effect on low-cycle fatigue resistance. X-ray diffraction was used to measure the surface and in-depth stress distributions. The prominent features of laser shock processing have been studied by an analytical approach to the main physical phenomena occurring successively during the impact. This led to an adequate treatment of conventionnal cylindrical low-cycle fatigue specimens. Fatigue tests were then conducted on Astroloy at 550°C. These showed the beneficial effect of laser shock processing.

Nomenclature.

(x,y,z)	: cartesian coordinates	τ_e	: laser pulse length
(r,θ,z)	: cylindrical coordinates	τ_o	: plasma confinement length
t	: time	d_P	: laser power density
$\overline{\overline{\sigma}}$	: stress tensor	$\mathcal{R}$	: radius of the irradiated zone
$\overline{\overline{\varepsilon}}$	: strain tensor	λ,μ	: Lamé coefficients
$\overline{\overline{\varepsilon}}^p$	: plastic strain tensor	α	: longitudinal wave velocity
L	: X-ray diffraction peak width	β	: transversal wave velocity
σ_Y	: yield strength	c_R	: Rayleigh wave velocity

$\sigma_{HEL} = (1+\lambda/2\mu)\ \sigma_Y$: Hugoniot elastic limit

Introduction.

The superalloys used in the aeronautic industry often work at the limit of their capacities. For example, in the case of Ni-based superalloys, such as "Astroloy" studied by the French aero engine manufacturer SNECMA as a test material for turbine discs, one of these limits is its fatigue resistance. Fatigue cracks generally initiate at defects such as inclusions or porosities : when the defect is located in the bulk material, it is not considered as damaging as a surface defect. So, the enhancement of the capabilities of an engine part can only be achieved if all risks of early fatigue failure (by surface crack initiation) are eliminated. This can be achieved by an adequate treatment of the surface of the engine part to protect the material against these damaging defects.

Shot peening is the surface treatment currently used by SNECMA. It induces superficial residual stresses that counteract the applied stress during fatigue loading, thus reducing the harmfulness of the defects. However, although efficient, shot peening exhibits several

disadvantages such as possible superficial particle inclusions, problem of accessibility to certain areas and surface roughness modification. These problems can be overcome by using the laser shock treatment, i.e. "laser peening". Laser peening treats a larger surface volume than shot peening [1], and so offers protection to a greater depth against defects of larger sizes.

Principles of laser shock treatment.

The laser generated shock mainly results from a mechanical phenomenon based on a shock wave created by an explosion of laser-irradiated matter. When a material is exposed to a laser beam with a sufficiently high fluence, a fine layer evaporates thus forming a plasma. The pressure of the plasma (up to a few GPa) creates a shock wave which propagates within the material (Fig.1). To induce this phenomenon, a short-pulsed laser must be used in order to reach a sufficiently high power density : a power density of 10^{13} $W.m^{-2}$, which is required typically, corresponds to pulse lengths between 100 ps and 100 ns.

In order to prevent the material surface from damage during the treatment, the target material is covered by a protective overlay such as a black adhesive film or a metal foil. Thus, the plasma is created by the overlay with detrimental effects such as thermal effects, ablation or matter projection, affecting only the protective overlay. Only the mechanical shock wave is therefore transmitted to the material.

The material is also covered by a "confining" transparent overlay such as water : the plasma then forms in the confined volume between the confining overlay and the surface, and its expansion in the direction perpendicular to the surface is dramatically limited. The pressure of the plasma is thus magnified and its decay time is increased by a factor of 2 to 3 compared to the pulse length.

After the shock wave is created at the surface, it propagates through the bulk material as a uniaxial plane wave. The state of deformation at the passage of this stress wave is uniaxial and, if the vertical stress σ_{zz} is greater than the Hugoniot Elastic Limit σ_{HEL} (or yield strength in uniaxial deformation state), plastic flow occurs (Fig.1). Since the shock wave is compressive, plastic deformation is negative, i.e. compressive, along the direction of propagation (or z-axis) while it is positive, i.e. tensile, along the direction parallel to the surface or perpendicular to the direction of propagation (that is the r- or θ-axis).

After the shock wave, the material returns to equilibrium for which the stresses parallel to the surface are compressive due to the reaction of the surrounding undeformed matter.

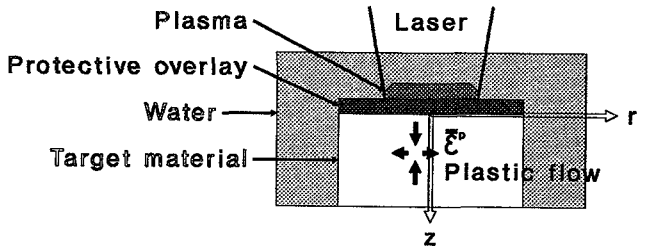

Figure 1 : Principle of laser shock treatment and cylindrical coordinate system.

Materials and apparatus.

The aeronautical Ni-based superalloy used is P/M (Powder Metallurgy) polycrystalline Astroloy (NKi7CDAT in the French standards) for turbine discs. Its composition is given in Table 1. Its yield strength σ_y at room temperature is about 1050 MPa. Astroloy samples consist of mirror-polished 2 x 2 x 1 cm^3 parallelepipeds and 4.37 mm-diameter cylindrical specimens for fatigue testing.

The laser shock experiments were conducted using the Nd-glass lasers of the L.U.L.I. laboratory of the "Ecole Polytechnique" and the L.A.L.P. laboratory of the "Etablissement Technique Central de l'Armement". The pulse length is τ_e = 25 ns approximately. The first laser delivers highly homogeneous laser beams of up to 150 J but with a pulse repetition rate of 1 every 20 min, while the second one delivers only an energy of 80 J at every pulse but the pulse repetition rate is up to 1 every minute. The beams are focused using spherical or cylindrical lenses to form 8 mm-diameter cylindrical spots or 16 x 4 mm^2 elliptic spots.

The laser power density d_p is then about 5 GW.cm^{-2}.

Residual stress measurements are made by X-ray diffraction. The wavelength λ_o = 1.02 Å of the Mn K_α radiation is diffracted by the {311} planes of nickel at an angle $2\theta \simeq 153°$. In depth measurements are determined by electro-polishing the surface of the samples down to given depths. The measured values are then corrected to take into account the stress relaxation due to the modification of the stress boundary conditions.

Table 1 : Chemical composition (wt.%) of Astroloy.

Co	Cr	Mo	Al	Ti	Zr	C	B	Ni
16.6	14.8	5.0	3.8	3.5	0.04	0.015	0.02	bal.

In-depth residual stress measurements.

The in-depth profiles show that residual stresses remain negative, i.e. compressive, up to 1 mm in depth (Fig.2). Outside of the center of the impact, for example for r = 3 mm, the superficial residual stress reaches -500 to -700 MPa for the most efficients shots [1]. This order of magnitude is in agreement with results on different materials for which it is generally claimed that the maximum superficial residual stress that can be obtained is a little more than half the yield strength.

In-depth profiles at the very center of the impact (r = 0) will be discussed later.

Whereas the residual stress becomes zero for z = 1 mm, the depth of material plastically affected by the shock is greater (about 1.5 mm). This value can be determined in two ways. It corresponds to the value of z where the measured residual stress (without any correction for relaxation) reaches zero : beyond this depth, the metal is not plastically deformed, therefore at equilibrium after electro-polishing of the upper layer. This can also be obtained from the curves of the X-ray diffraction peak width determined during the measurements. The peak width is actually caracteristic of the plastic deformation rate within the material. Thus, the peak width decreases with depth as does the plastic deformation, until it stabilizes after z = 1.5 mm at the value of undeformed matter.

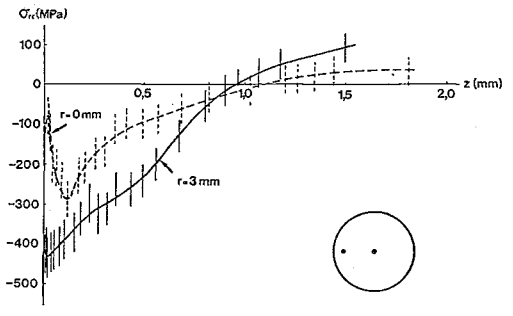

Figure 2 : In-depth residual stresses profile.

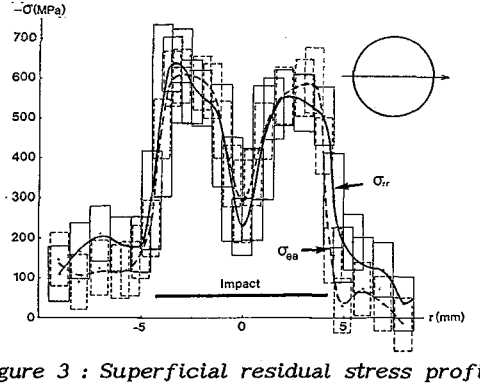

Figure 3 : Superficial residual stress profile.

Surface residual stress measurements.

Superficial residual stress profiles along diameters of circular impacts always lead to the same conclusions. According to the cylindrical symmetry of the problem, the radial and orthoradial stresses, i.e. σ_{rr} and $\sigma_{\Theta\Theta}$, are found to be the two non zero eigenvalues of the stress tensor.

Except at the very center of the impact (r = 0), the compressive stress distribution is almost uniform in the impact (Fig.3). But in a small area right in the center of the impact (for r ≤ 0.5 mm), the residual stress level almost decreases to zero. This now well-known phenomenon is independant of the laser and occurs for a circular impact whatever the irradiation conditions. This stress drop is clearly a superficial phenomenon since in-depth measurements show that the difference between the center (r = 0) and the

surrounding area (e.g. r = 3 mm) almost disappears below a depth of 0.2 mm. It is attributed to a state of plastic deformation created by release waves that acts against the plastic deformation left by the shock wave. However, although this phenomenon has long been described empirically, the exact mechanism by which it is produced has only been understood since adequate mathematical models have been developed in the past few years [2].

Description of the wave propagation during a shock experiment.

Modeling of the wave propagation due to a laser shock have been conducted using methods of resolution of Lamb's problem. These methods are applied to a perfectly elastic material loaded by a uniform pressure within the circular impacted area during a length τ_o. They consist of the resolution of the equation of motion (or Lamé - Clapeyron equation) using Fourier and Hankel [3] or Laplace and Hankel [4] transforms. The exact analytical solution can be used to evaluate the kind of plastic deformation created in the case of an elasto - plastic material, simply by considering that this solution is applied everywhere to the material as a path of loading in the deformation (or $\bar{\bar{\varepsilon}}$-) space [2]. The chronology of the laser shock experiment is developed below (Fig.4).

From t = 0, i.e. when the plasma pressure is applied to the material, a plane longitudinal wave is created at the surface. This plane wave propagates in the vertical or z-direction. It induces plastic deformation of the form :

$$\bar{\bar{\varepsilon}}^{P} = \begin{pmatrix} \varepsilon^{P} & 0 & 0 \\ 0 & \varepsilon^{P} & 0 \\ 0 & 0 & -2\varepsilon^{P} \end{pmatrix} \quad \text{with } \varepsilon^{P} > 0$$

However, at the border of the impact, release waves are created. They consist of two types of waves : a longitudinal or P-wave which corresponds to an edge effect due to the impossibility for a discontinuity to exist between the inner and the outer sides of the impact, and a transversal or S-wave which is created by the shear ε_{rz} that occurs at the side of the impact and that induces the cliffs that define the crater of the process zone.

After the plasma dissipates, all waves continue to propagate. The plane wave keeps propagating towards the interior and looses energy by plastic deformation. Both the release P- and S-waves leave the impact boundary and propagate along torus-like wave surfaces, the first being at the longitudinal velocity $\alpha = \sqrt{(\lambda+2\mu)/\rho} \simeq 6000$ m.s^{-1} and the second at the transversal velocity $\beta = \sqrt{\mu/\rho} \simeq 3300$ m.s^{-1}. The P-release wave interacts with the sample surface z = 0 to create a "head wave" but the amplitude of both is too low to have any permanent (i.e. plastic) effect thereafter. On the other hand, the S-release wave strongly interacts with the surface to form a Rayleigh wave. Since the latter is a surface wave, its energy is radiated horizontally at a velocity $c_R \simeq 3100$ m.s^{-1} and is thus confined along the surface. The amplitude of the Rayleigh wave thus decreases very slowly.

When at time $t = \mathcal{R}/c_R$, all the Rayleigh waves created from the boundary $r = \mathcal{R}$ reach the center r = 0, they all superpose or "focus" and the amplitude of the corresponding strain field $\bar{\bar{\varepsilon}}^{RAY}$ increases dramatically. The Rayleigh wave has the two components : a P- or longitudinal type and a S- or transversal type. Calculations show that the P-component of the Rayleigh wave creates plastic deformation of the type :

$$\bar{\bar{\varepsilon}}^{RAY-P} = \begin{pmatrix} \varepsilon^{P} & 0 & 0 \\ 0 & \varepsilon^{P} & 0 \\ 0 & 0 & -2\varepsilon^{P} \end{pmatrix} \quad \text{with } \varepsilon^{P} < 0$$

It then tends to annihilate the plastic deformation left by the plane wave near r = 0. The S-component leaves a shearing plastic deformation of the type :

$$\bar{\bar{\varepsilon}}^{RAY-S} = \begin{pmatrix} 0 & 0 & \varepsilon^{P}_{rz} \\ 0 & 0 & 0 \\ \varepsilon^{P}_{rz} & 0 & 0 \end{pmatrix}$$

where ε^{P}_{rz} is approximately a linear fonction of r for $r < c_R\tau_o/2$. This consequently induces a V-shape plastic deformation of the surface near the center. After the passage of the Rayleigh wave, the underlying matter reacts against the deformation of the Rayleigh wave affected layer and tends to flatten the V then opening its vertex and creating tensile stresses σ_{rr} and $\sigma_{\Theta\Theta}$ for $r < c_R\tau_o/2$.

So, the stress drop at the center of the impact is due to the effects of both the P- and S-components of the Rayleigh waves which are emitted at the same distance of the center

for r = $\mathcal{R}$ and which reach the center at the same time.

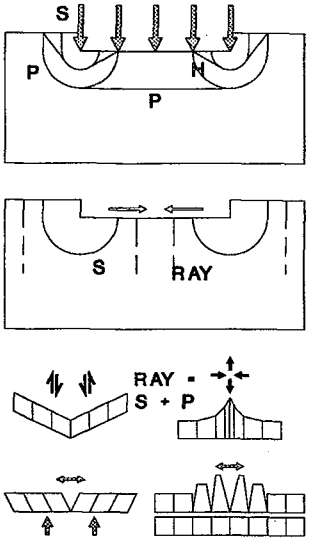

Emission of :

Plane wave P

Release waves P and S

Interaction of the P - release wave with the surface ⟶ Head wave H

Interaction of the S - release wave with the surface ⟶ Creation of the Rayleigh wave RAY

Propagation of the Rayleigh wave

Focussing of the Rayleigh wave

⟶ Plastic flow of the affected layer

Creation of the residual stresses at the center

Figure 4 : Chronology of laser shock treatment.

Advantages due to the use of elliptic impacts.

The interest from elliptic impacts is two-fold. First, an elliptic shape is more suitable for treating elongated specimens like fatigue specimens. Second, it drastically reduces the amplitude of the stress drop by limiting wave focussing. For an elliptic impact, release therefore Rayleigh waves are emitted from the elliptic boundary. Then they can not meet altogether at the same point at the same time. In fact, the convergence of the Rayleigh waves occurs along the whole long axis x of the ellipse, with no focussing effect. The stress drop is consequently minimal and affects the stress component σ_{yy} in the direction parallel to the small axis y (Fig.5). The small stress drop near the center of the impact, which also corresponds to a diffraction peak width drop, can not be attributed to a similar effect but to an area where the laser intensity is smaller due to diffraction effects of the laser light during focussing.

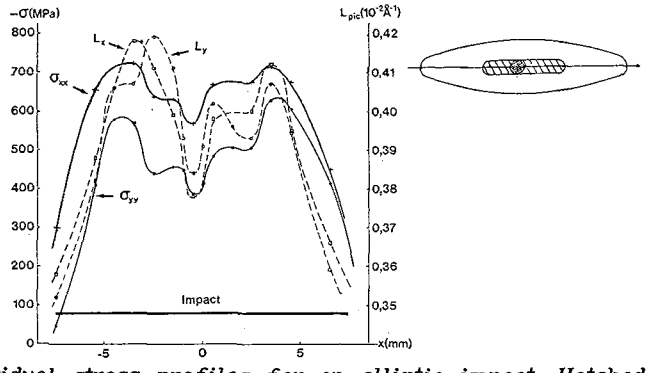

Figure 5 : Superficial residual stress profiles for an elliptic impact. Hatched areas are the stress drop locations.

Fatigue tests.

Treating of the fatigue specimens is achieved using 4 elliptic impacts along each of 6 generating lines of the specimen. The whole surface of the cylindrical portion of the specimen is then completely treated. The mean stress value on the surface are σ_{zz} = -400 MPa and $\sigma_{\Theta\Theta}$ = -700 MPa (Fig.6).

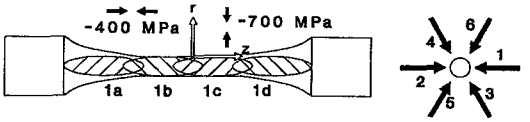

Figure 6 : Sequence of treatment for a fatigue specimen.

Fatigue tests have been conducted by SNECMA at the service temperature (T = 550°C), the applied stress σ oscillating from 0 to the maximum stress σ_{max} at a frequency of 0.5 Hz.

For σ_{max} = 1000 MPa, no failure is observed (Fig.7). For σ_{max} = 1150 MPa, only one early superficial failure (at 6000 cycles) and one internal failure (at 40000 cycles) are observed. The other 3 specimens did not fail for over 200000 cycles. Every unfailed specimen was further tested at σ_{max} = 1200 MPa where early failures always occurred. The large increase of fatigue life shows a beneficial effect of laser shock treatment that is actually due to a protection against superficial defects since those defects led to failure at σ_{max} = 1200 MPa. However, these results over a small number of tests need to be confirmed by further tests.

For σ_{max} = 1200 MPa (whether directly or after a first test at σ_{max} = 1000 or 1150 MPa), early superficial failure always occurred as for untreated specimens. The compressive residual stresses induced by laser shock treatment probably relax very soon by such a high applied stress.

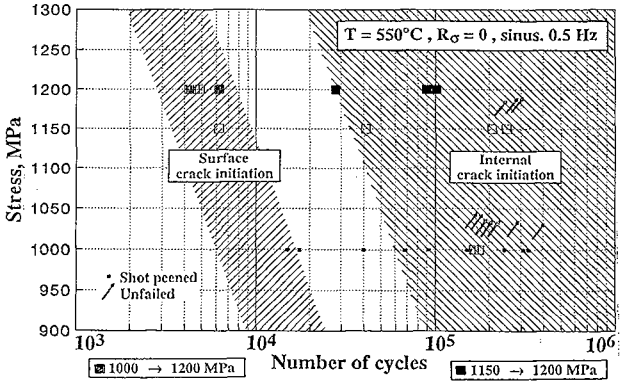

Figure 7 : Fatigue tests results.

Conclusion.

Adopting a rationnal approach to understand the mechanisms involved during a laser-generated shock led to designing and applying an homogeneous treatment to fatigue specimens. The beneficial effect of laser peening has been shown. Further fatigue tests to determine residual stress relaxation for the various applied stresses are in program.

Acknowledgements.

This study has been supported by the "Direction des Recherches Etudes et Techniques (DRET)" under contract # 87.017.010.16 and 92.017.00.003, which is gratefully acknowledged. The authors would also like to thank Messrs. Lebrun and Ji for technical assistance and helpful discussion.

Bibliographie.

[1] FORGET P. et al., *Mat. & Manuf. Proc.* 5(1990)501.
[2] FORGET P. and JEANDIN M., Proc. of "Colloque Contraintes Résiduelles", 22-23 Sept. 1992, Arcueil, DRET/ETCA pub., Arcueil, France, (1992)9.
[3] AKI K. and RICHARDS P.G., in "Quantitative Seismology", A. Cox ed., W.H. Freeman and Co, New York, NY, U.S.A., (1980)304.
[4] EASON G., *J. Inst. Maths Applics* 2(1966)299.